The comparison of discrete ordinate and Monte Carlo methods in solving of the radiation transfer equations in a heterogenous reactor

G. Asadollahfardi, M. Noori, M. Asadi and M. Taherioun

ABSTRACT

Photoreactor applications in water and wastewater treatment has been increased in recent years. The simulation of radiation distribution inside the reactors allows the optimization of its operation. The radiation transfer equation (RTE) illustrates the field radiation. We applied the discrete ordinate (DO) method to solve the RTE and computed the local volumetric rate of energy absorption (LVREA) in a photoreactor, consisting of a Ultra Violet (UV) lamp and titanium dioxide Degussa P25 (TiO_2 DP 25) catalyst. First, GAMBIT 2.4.6 was employed to model the reactor in three dimensions. The simulation of the radiation distribution was carried out using FLUENT 14.5 software in the framework of a multiple point source summation (MPSS) model. The robustness of the DO approach was assessed by comparing with the Monte Carlo (MC) method and experimental data. The coefficient of determination (R^2) and index of agreement (IA) of DO and experimental data were 0.95 and 0.93, respectively. The DO and MC had a good convergence in the low concentrations of TiO_2 DP 25. In the concentrations between 0.03 g/l to 0.15 g/l, the difference with experimental data increased. In the concentration of 0.15 g/l, and beyond, the both methods and experimental data were in a good agreement.

Key words | discrete ordinate (DO) method, Monte Carlo (MC) method, photoreactor, radiation transfer equation (RTE), ultraviolet (UV) lamp

G. Asadollahfardi (corresponding author)
M. Noori
Civil Engineering Department,
Kharazmi University,
Tehran 15719-14911,
Iran
E-mail: *asadollahfardi@yahoo.com*

M. Asadi
Engineering Department,
University of Saskatchewan,
Saskatoon S7N 5A9,
Canada

M. Taherioun
Civil Engineering Department,
Isfahan University of Technology,
Isfahan,
Iran

INTRODUCTION

Urbanization, population growth, and escalating water consumption are associated with new challenges in the management of water resources. Due to the overall load and insufficient elimination of some pollutants, advanced water, and wastewater processes become progressively applicable. In recent years, advanced oxidation processes application in removing non-biodegradable compounds in water and wastewater has been increased (Wols & Hofman-Caris 2012). In the AOTs (advanced oxidation technologies), ultraviolet (UV) radiation as well as ozone (O_3), hydrogen peroxide (H_2O_2), photocatalysts and metal catalysts can be used to generate highly reactive hydroxyl radicals to oxidize the target pollutants. Photocatalysis processes use solid semiconductors that are activated by UV light. Titanium dioxide (TiO_2) is considered as one of the most widely used photocatalysts. This approach is non-toxic, economical, highly photochemically and chemically stable and eco-friendly. To evaluate and optimize the performance of photodegradation with TiO_2 catalysts, a deeper understanding of the mechanistic models, the radiation distribution, reactor hydraulics, and intrinsic TiO_2 photo-oxidation kinetics are vital (Turolla *et al.* 2016). An optimized UV/TiO_2 photocatalystic oxidation generates hydroxyl radicals at adequate concentrations.

Radiation distribution is one of the indispensable parameters in the simulation of photoreactors (Elyasi & Taghipour, 2005). The radiation transfer equation (RTE) depicts the radiation distribution and can be solved using various methods (Cassano *et al.* 1995). Because the experimental and pilot studies for UV/TiO_2 photoreactors are

doi: 10.2166/aqua.2017.058

time consuming and expensive procedures, the mathematical methods (such as finite volume and Monte Carlo (MC) technique and discrete ordinate (DO) method) have been developed to solve the RTE. The mentioned methods can cause a reduction in the number of experimental works and pilot studies. In this regard, several studies have been conducted.

Peyton & Glaze (1988) designed a model of ozone degradation using UV lamps. Crittenden *et al.* (1999) proposed a model of reaction kinetics and assumed that the net formation rate of free radical species was not zero. Bolton (2000) considered a model of multiple point source summation (MPSS) to study the refraction of UV in various environments including air, water and quartz. As he did not consider the refraction, the results were unreliable and error reached 25%. Liu *et al.* (2004) depicted that the DO model considerably overvalued the radiation distributions in the near-lamp regions, but undervalued the radiation distributions in the near-wall areas. Jin *et al.* (2005) studied the shadow and reflection effects of the four lamps on a reactor. As they did not consider the shadow, the rate of radiation distribution reached 33% more than real values.

Taghipour & Sozzi (2005) studied the hydrodynamics of a UV reactor. They verified the results using the velocity profile attained by a particle image velocimetry test. Sozzi & Taghipour (2006) evaluated UV reactor performance modeling using Eulerian and Lagrangian methods. They encompassed effective factors such as reaction kinetics, the particular hydrodynamic of the reactor and the model of radiation distribution. They reported a good agreement in the attained results at high flow rate. Munoz *et al.* (2007) predicted the performance of UV disinfection sensitivity to particle tracking inputs using computational fluid dynamics (CFD). The reactor encompassed the middle pressure lamps in water treatment. They depicted that the rate of inactivation kinetics was dependent on the model meshing (tetrahedral and hexagonal) and the selection of the turbulence model was less sensitive to meshing.

Imoberdorf *et al.* (2008) employed the MC approach to simulate radiation field in homogeneous photoreactors with one, two and three lamps. The results were in a good consensus with experimental perceptions. The reflection, refraction and absorption of photons by the lamp and wall were of great importance in the radiation field. Furthermore, 100% opaque lamp assumption worked for reactors with non-reflective walls. Ho (2009) reported that the DO was able to account for the shadowing, reflection and refraction of the modelled geometry in RTE solving. Elyasi & Taghipour (2010) simulated a UV photoreactor in degradation of chemical contaminants. They solved the governing equations on the performance of a UV reactor.

Imoberdorf & Mohseni (2012) applied MC approach in solving RTE to simulate vacuum-UV photoinduced breaking down of the herbicide 2, 4-dichlorophenoxyacetic acid. Li *et al.* (2013) compared experimental and model results to study radiation distributions in a UV reactor. They reported shadowing effect in totally and partially blocked regions. When the UV lamps were placed near the reactor wall, reaction from the wall was strong. Zhang & Anderson (2013) studied destruction of a chlorinated aromatic compound by UV photolysis and investigated using advanced oxidation for air emission treatment. They indicated a photoreactor is more efficient at high concentration of the organic pollutant. Li *et al.* (2013) represented an enhanced real-time fluence monitoring technique to run UV reactors. They stated that this method significantly reduced the number of biodosimetry examinations while increasing the monitoring accuracy.

Asadollahfardi *et al.* (2014) compared the UV radiation intensity between a single and double lamp in a photoreactor to evaluate the water disinfection. The power of the reactors was the same. DO method was used to solve RTE through FLUENT software. They demonstrated that the performance of a single lamp was more reliable than the reactor with two lamps. Bagheri & Mohseni (2014) applied CFD to a model vacuum-UV/UV photoreactor. DO method was employed to solve RTE. The reflection, refraction and absorption of photons by the wall and slurry medium was regarded in the radiation modeling. The results showed that the higher absorption coefficient of water drove a significant attenuation of radiation, particularly for UV lamps with lower wavelength. Li *et al.* (2017) studied the impact of wall reflection on annular single-lamp UV reactor performance. The UV distribution was simulated using a calibrated DO. The radiation distribution was directly dependent on the wall reflectivity. They reported that the DO performance in solving the RTE was precise and reliable.

The radiation dispersion is paramount in reactor simulations and influences in the inactivation rate of

microorganisms. Due to the literature review, the evaluation of DO method reliability in RTE solving is vital. We studied the radiation dispersion for the photocatalytic degradation of phenol. Therefore, the main objective of the manuscript was to assess the results of DO method in different concentrations of titanium dioxide (TiO_2) catalyst for solving the RTE and find out the reliability of the DO technique in comparison with Monte Carlo (MC) predictions and experimental data, which were from Moreira del Rio (2011).

METHODS

The effective factors in a UV system are as follows: hydrodynamics of the reactor, RTE, reaction kinetics (including oxidation of chemical pollutants and the inactivation rate of microorganisms), and internal features of the reactor (Elyasi 2009). The RTE simulates the light intensity dispersion inside the reactor. The light intensity dispersion is dependent on the following items: type of lamp, the position of lamp, reactor geometry, catalyst type, catalyst concentration, particle agglomeration size, the reflecting specification of reactor walls, inflow rate, pH, outflow rate, and radiation wavelength (Salaices *et al.* 2002; Pareek *et al.* 2003; Kheyrandish *et al.* 2017). For each directional unit vector (Ω) at a specific wavelength (λ), the RTE indicates the radiation field. (Equation (1)) (Martin *et al.* 1996; Brandi *et al.* 2003; Pareek *et al.* 2003, 2008; Marugán *et al.* 2006).

$$\nabla[\Omega I_\lambda(\mathbf{s},\Omega,t)] = k_\lambda(\mathbf{s},\Omega,t)I_\lambda(\mathbf{s},\Omega,t) + \sigma_\lambda(\mathbf{s},\Omega,t)I_\lambda(\mathbf{s},\Omega,t) + j_\lambda(\mathbf{s},t) + \frac{1}{4\pi}\sigma_\lambda(\mathbf{s},t)\int_{\Omega'=4\pi}\psi(\Omega'\Omega)I_\lambda(\mathbf{s},\Omega',t)d\Omega' \quad (1)$$

where **s** is position vector; Ω is a directional unit vector; t is time (s); $I_\lambda(\mathbf{s},\Omega,t)$ is radiant intensity for specific solid angle Ω and specific location **s**; k_λ is absorption coefficient of the medium (l/m); σ_λ is scattering coefficient of the particulates in the medium (l/m); j_λ is radiation emission (W/sr·m^2); $\psi(\Omega'\Omega)$ is phase function. $k_\lambda(\mathbf{s},\Omega,t)I_\lambda(\mathbf{s},\Omega,t)$ represents the loss of photons due to absorption, $\sigma_\lambda(\mathbf{s},\Omega,t)I_\lambda(\mathbf{s},\Omega,t)$ describes the loss of radiation due to out-scattering, $j_\lambda(s,t)$ describes the emission of light due to the temperature, $(1/4\pi)\sigma_\lambda(\mathbf{s},t)\int_{\Omega'=4\pi}\psi(\Omega'\Omega)I_\lambda(\mathbf{s},\Omega',t)d\Omega'$ illustrates the gain in radiation due to in-scattering. In the lack of emission (operating at relatively low temperature) and scattering (no significant concentration of particulates), Equation (1) can be simplified to Equation (2) (Elyasi & Taghipour 2010).

$$\frac{dI(s,\Omega)}{ds} + k(s,\Omega)\,I(s,\Omega) = 0 \quad (2)$$

The local incident radiation at any point from all the directions is defined by Equation (3):

$$G(x,y,z) = \int_0^{\Omega=4\Pi} I_\lambda(s,\Omega)d\Omega \quad (3)$$

Equation (3) facilitates the developing of a radiation distribution model for any type of radiant point source. To solve RTE, two issues have to be defined: the optical specifications (such as absorption and scattering coefficients and the phase function) and the boundary circumstances (Pareek *et al.* 2003). Following this, the local volumetric rate of energy absorption (LVREA) at any point can be achieved using Equation (4).

$$\text{LVREA}\,(x,y,z) = k_\lambda G_\lambda(x,y,z) \quad (4)$$

The DO can be used to compute the radiation intensity due to absorption, scattering and emission within the fluid, as well as reflection and emission from the reactor walls. The approach splits up the radiation field into a number of separate directions and solves the RTE for each of these directions. The DO modifies Equation (1) for radiation intensity in the spatial coordinates (x, y, z). In other words, the model solves the RTE for a limited number of discrete solid angles in the vector direction Ω fixed in the coordination of (x, y, z) (Equation (5)).

$$\nabla[I(s,\Omega)s] + (k_\lambda + \sigma_\lambda)I(s,\Omega) = k_\lambda n^2\frac{\sigma T^4}{\pi} + \frac{\sigma_\lambda}{4\pi}\int_0^{4\pi} I(s,\Omega')\psi(\Omega'\Omega)d\Omega' \quad (5)$$

The perfect description of DO method would be found in Stamnes *et al.* (1988) and Liou & Wu (1996). The method is implemented within the FLUENT CFD code, a commercial computational fluid dynamics software package.

The MC method is a statistical approach that can be deployed to solve RTE. MC traces individual photon(s) from their source (dependent on releasing power of the

lamp) till either absorbed by solid particles and reactor walls or scattered in the system (Yokota *et al.* 1999; Pareek *et al.* 2003). When a photon is absorbed (based on absorption coefficient), a new photon will be released in a random direction. The direction is chosen based on scattering coefficient of the medium. The non-absorbed photons will reach the walls. Given the specifications of the wall, the photons might be reflected or absorbed. In the MC method, the emission, reflection and absorption in the photocatalysis are considered accidental events, which may occur at each point. Hence, the optical characteristics of the medium and phase function are determinative to develop the probability dispersion functions for each event. The ideal number of events in developing the MC approach could be the total number of released photons. The perfect description of the MC method can be found in Pareek *et al.* (2008) and Moreira del Rio (2011).

The simulated photoreactor, which included TiO_2 Degussa P25 (DP 25) catalyst, was based on the described reactor in Moreira del Rio (2011). The height, internal and external radii of the reactor were 44.5, 1.76 and 4.44 cm, respectively. The internal Pyrex™ glass thickness was 0.23 cm. The illuminated reactor volume was 2.5 L. The lamp used in the photoreactor is a 15-W 1.33 cm radius, 41.3 cm length, blacklight UV lamp. The emission range varied between 300 and 420 nm. The emission rate was 1.910×10^{-5} Einsteins/s. The physical feature of the reactor is depicted in Figure 1 (Moreira del Rio 2011). The following elements formed the reactor: (1) 15 W black light lamp; (2) Pyrex glass inner tube with diameter of 3.58 cm; (3) replaceable Pyrex inner tube with diameter of 5.6 cm; (4) silica windows; (5) black polyethylene outer tube; (6) stirred tank; (7) centrifugal pump; (8) air injector; and (9) sampling port.

We modeled the reactor with various concentrations of TiO_2 DP25. First, GAMBIT 2.4.6 software was employed to create the geometry of the reactor and mesh it. Figure 1 depicts the geometry of the reactor. The geometry was combined using 134,294 tetrahedral cells and 26,921 nodes. The suitability of the geometry in FLUENT can be evaluated using an index of Minimum Orthogonal Quality, which varies between 0 (low aptness) to 1 (high aptness). Our index was 0.95, which was acceptable. The MPSS was used to simulate the radiation of the lamp. FLUENT 14.5 software (2012), which is based on finite volume, was used to solve the RTE. For reactor simulation, the following initial assumptions were made (Moreira del Rio 2011): UV lamp was used as a uniform emission source; the flow was steady state; the inflow to the reactor was 15 L/min; the initial concentration for different experimental work was prepared from

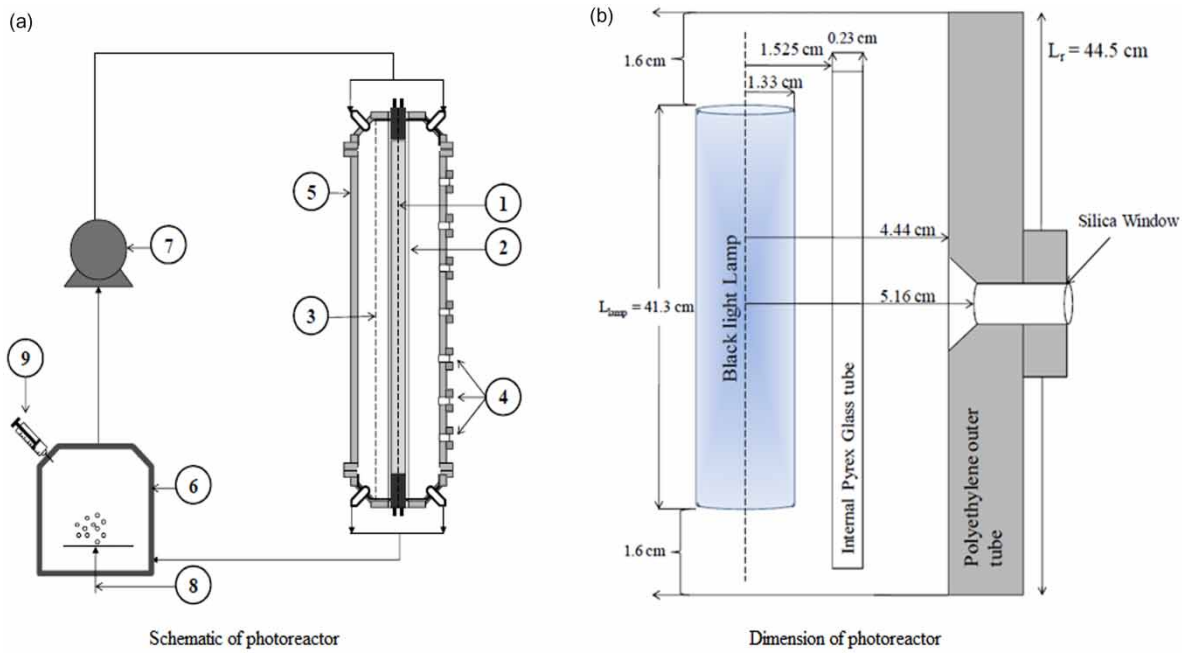

Figure 1 | The photoreactor (Moreira del Rio 2011).

a stock solution of 2,400 ppm of C phenol; the pH was adjusted to 3.7 ± 0.1 using sulphuric acid solution; the temperature was 30 ± 1 °C; the properties of the fluid in the reactor were as follows: thermal conductivity = 0.6 W/(m K), viscosity at 20 °C = 0.001 Pa·s, absorption and scattering coefficients were computation based and were 32 and 280(1/m), respectively; the properties of Pyrex sleeve were as follows: density = 2,230 kg/m^3, specific heat = 750 J/(kg K), thermal conductivity = 0.5 W/m K, absorption coefficients (1/m); Turbulent intensity = 5% and hydraulic diameter = 2.66 cm. Mass flow rate = 0.25 kg/s.

As indicated in Figure 2, the photoreactor contains seven circular windows, including S1-UV grade fused silica, 0–32 cm thickness × 2.54 cm diameter. These windows permit radiation transmission measurement through the annular section of the photoreactor. Radiation transmission through the different TiO_2 catalyst with different concentrations measured by a Stellar Net EPP2000C-25 LT16 spectrometer (Moreira del Rio 2011). To measure the radiation, a UV-opaque and inner polished collimator was attached to the photoreactor windows to limit the rate and the angles of the radiation transmitted through the catalyst suspensions. Moreira del Rio (2011) also used UV-opaque collimator including 2.3 cm length × 1 cm diameter, angle of 44.4° to find out the extinction coefficients because their non-reflecting surface minimizes the forward-scattering radiation reaching the detectors. An aluminum polished collimator comprising 2.3 cm length × 1 cm diameter, angle view of 160° permitted the assessment of total transmitted radiation through the slurried medium.

The MPSS considers the lamp as a light source, which has radiation in all directions. The effect of UV radiation at each point can be attained by the sum of the energy of every single point source (Equation (6)).

$$E(r, z) = \sum_{i=1}^{n} \frac{(p/n)}{4\pi l_i^2} \exp\left[-\sigma_w (r - r_L) \frac{l_i}{r}\right] \quad (6)$$

where n is the number of sources; z is the axial distance (m), and l_i is the distance from the current location to the point source number (m).

The scattering and absorption coefficients for TiO_2 DP25 are dependent on the wavelength of the light. The RTE should be solved for every wavelength separately, which is a time consuming process. Therefore, the mean values of wavelengths were considered to acquire the coefficients (Equations (7) and (8); Moreira del Rio 2011).

$$\kappa = \kappa_\lambda^* W_{cat} \quad (7)$$

$$\sigma = \sigma_\lambda^* W_{cat} \quad (8)$$

where κ_λ^* is the specific absorption coefficient (1/m); σ_λ^* is the specific scattering coefficient (1/m) and W_{cat} is the solid catalyst loading (g/m^3). The values of κ_λ^* and σ_λ^* for TiO_2 DP25 can be obtained through Figure 3.

The emission range of the UV lamp was assumed to be 360 nm. Therefore, the amounts of k^* and σ^* were 0.6394 and 5.677, respectively. For the catalyst mass flow rate of

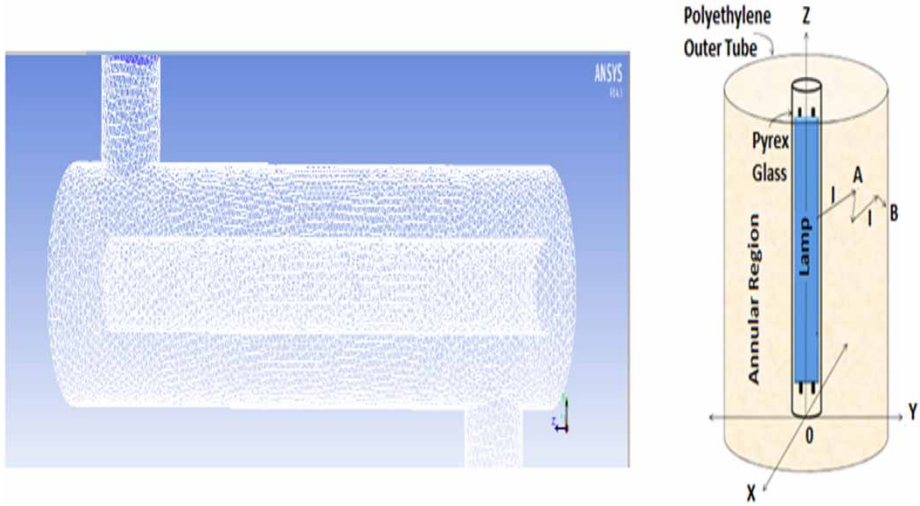

Figure 2 | The geometry of reactor.

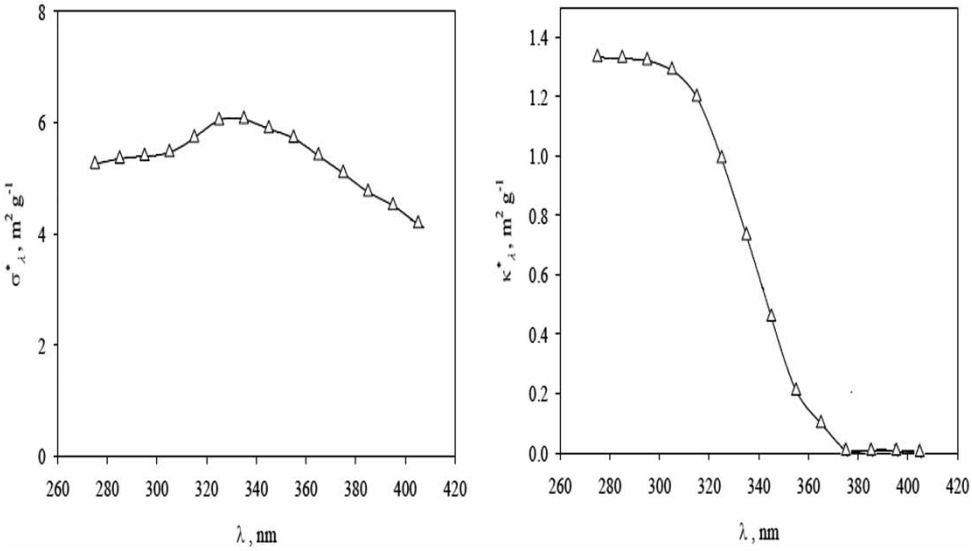

Figure 3 | Specific scattering and absorption coefficients for TiO_2-DP25 at wavelength of λ (Romero *et al.* 2003).

0.05 g/m^3, the scattering and absorption coefficient would be 32 m^{-1} and 280 m^{-1}, respectively.

The empirical LVREA can be obtained based on the total radiation transmission, the non-scattered radiation transmission and the backscattering radiation exiting the system. Moreira del Rio (2011) applied macroscopic balance to estimate empirical LVREA in different concentrations of TiO_2 DP 25. In this regard, the following steps should be taken. The perfect and detailed description can be found in Moreira del Rio (2011): the light source emission rate, which can be calculated based on the initial lamp emission rate, lamp decay coefficient and emission duration; rate of absorption of photons by the sleeve and inside of reactor; the absorbed light by TiO_2 – DP 25; rate of back-scattered photons in the reactor; rate of absorption of photons and experimental LVREA.

The next step was determining of boundary conditions (BCs) for the reactor in the simulation using FLUENT. The BCs arrangements were based on the empirical set up of Moreira del Rio (2011).

For solving the hydrodynamic equations of the photoreactor, as mentioned previously, we divided the total volume of the reactor into 134,284 tetrahedral cells by applying GAMBIT software then the results of the GAMBIT software were introduced to the FLUENT software. We selected pressure based on the FLUENT software because Much number was less than 0.8 and assumed steady state flow in the photoreactor. For the turbulence model, k-epsilon was applied because turbulence model does not significantly affect radiation domain. Influent flow was 15 l/min. Turbulent intensity was 5% and hydraulic diameter was 2.66 cm. Mass flow rate was 0.25 kg/s. Therefore, we solved the hydrodynamic equations of fluid and the RTE equation using FLUENT software. For CFD simulation, we considered the BCs of the reactor according to the empirical set up of Moreira del Rio (2011). The photon interactions with the reacting medium were determined by the absorption and scattering coefficients (Moreira del Rio 2011).

The BC type of lamp was regarded as semi-transparent. The outflow BCs, the internal emissivity for polyethylene was 0.92. The diffuse fraction changes between 0 (diffuse reflectivity) to 1 (specular reflectivity). Radiation around the circular lamp was heterogeneous. For simplicity, the reflection was assumed to occur at the same angle of the radiation. Therefore, we selected that the diffuse fraction for lamp and wall equalled 1. The BC type of external wall was opaque. The lamp was assumed as a semi-transparent material. We assumed the angles θ and ϕ of lamp and sleeve equal to 10^{-6} degrees. The diffuse irradiation of the lamp was 116 W/m^2. The sleeve around the lamp was Pyrex, which attracted 6% of the radiation. Therefore, the total radiation of lamp was 109 W/m^2.

We used a coefficient of determination (R^2) and Index of Agreement (IA) for the model efficiency (Equations (9) and (10)). The values of R^2 and IA vary between 0 and 1. If the values are close to 1, the model predictions are efficient and reliable. However, for values approaching 0, the model

results are inefficient and unreliable (Heckman 1979; Krause *et al.* 2005).

$$R^2 = \left(\frac{\sum_{i=1}^{i} (A_t - \bar{A})(F_t - \overline{F})}{\left(\sum_{i=1}^{n} (A_t - \bar{A})^2\right) \sum_{i=1}^{i} \left(\left(F_t - \overline{F}\right)\right)^2 \right)^{0.5} \Bigg)^2 \quad (9)$$

$$IA = d = 1.0 - \frac{\sum_{t=1}^{N} (A_t - F_t)^2}{\sum_{t=1}^{N} \left(|F_t - \bar{A}) + |A_t - \bar{A})\right|^2} \quad (10)$$

where A_t, F_t, $\bar{A}$ and $\bar{F}$ are observed (recorded) data, predicted data and average of observed data and the mean predicted data, respectively.

RESULTS AND DISCUSSION

The feasible effect of the Pyrex sleeve on the computations was evaluated. First, LVREA was calculated based on the presence of Pyrex sleeve and obtained 2.999×10^{-3} Einstein/m^3 s. Afterward, the calculation was carried out by ignoring the Pyrex sleeve and acquired 2.981×10^{-3} Einstein/m^3 s (Figure 4). The catalyst concentration was 0.05 g/l. The results depicted that the sleeve did not alter radiation dispersion.

The incident radiation had an inverse relation with the concentration of the catalyst. At a concentration of 0.05 g/l, the incident radiation varied between 8.867×10^{-5} and 1.34946×10^{-4} Einstein/m^2 s. While at a concentration of 0.2 g/l, the incident radiation was between 3.10345×10^{-5} and 3.39165×10^{-5} Einstein/m^2 s (Figure 5). The catalyst distribution in the reactor was uniform. Nonetheless, the radiation distribution near the wall was irregular. By increasing the catalyst concentration, more irregularity in radiation distribution was observed. The configuration of meshing in boundary layers may be effective in the radiation field (Figure 5).

Using the DO method and incident radiation at various concentrations of the catalyst, we computed the LVREA (Table 1). Our results had a good agreement with the experimental data, such that R^2 and IA were around 0.95 and 0.93, respectively (Figure 6). At TiO_2 concentrations between 0 to 0.03 g/l, a suitable convergence between the LVREA and experimental data was observed (Figure 6). At the concentrations between 0.03 g/l to 0.15 g/l, differences in the DO results and experimental data were detectable. At concentrations of 0.15 g/l and 0.20 g/l, considerable agreement was observed.

The evaluation of MC results with experimental data indicated that the R^2 and IA were 0.91 and 0.87. Similar to DO result, up to the concentration of 0.03 g/l, the experimental data and MC results were in considerable agreement (Figure 6). In the concentrations between 0.03 g/l to 0.15 g/l, the discrepancy between the predictions of MC and experimental data increased. Although the DO and MC results had an appropriate agreement with observations, the DO method resulted in more precise and robust outcomes (Figure 6). As indicated in Figure 6, between 0.03 g/l to 0.15 g/l of TiO_2 concentrations, the DO prediction of LVREA was more reliable than the MC prediction. As a general rule, application of the DO method for predicting LVREA is suggested.

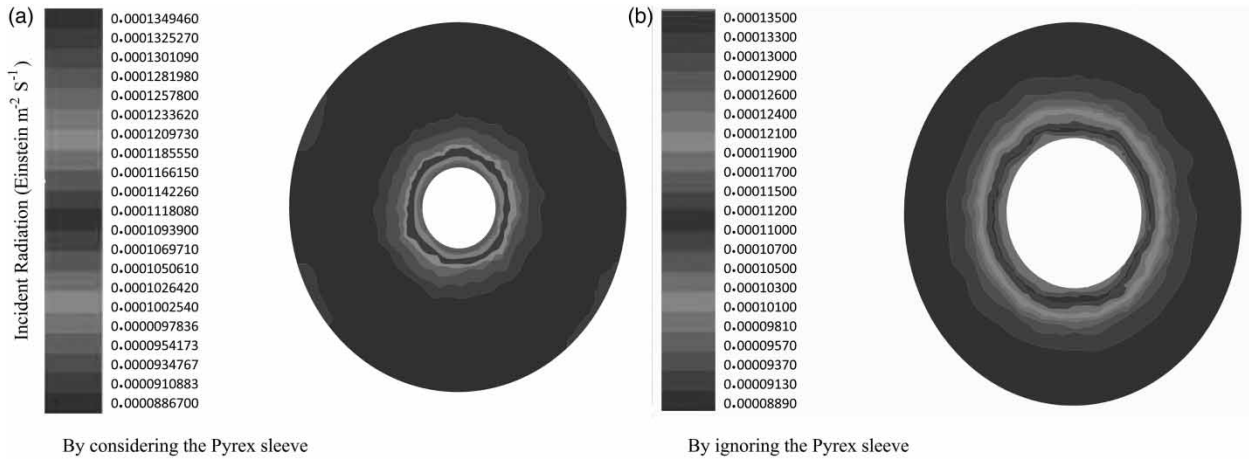

Figure 4 | The effect of the Pyrex sleeve in incident radiation at the catalyst concentration of 0.05 g/l.

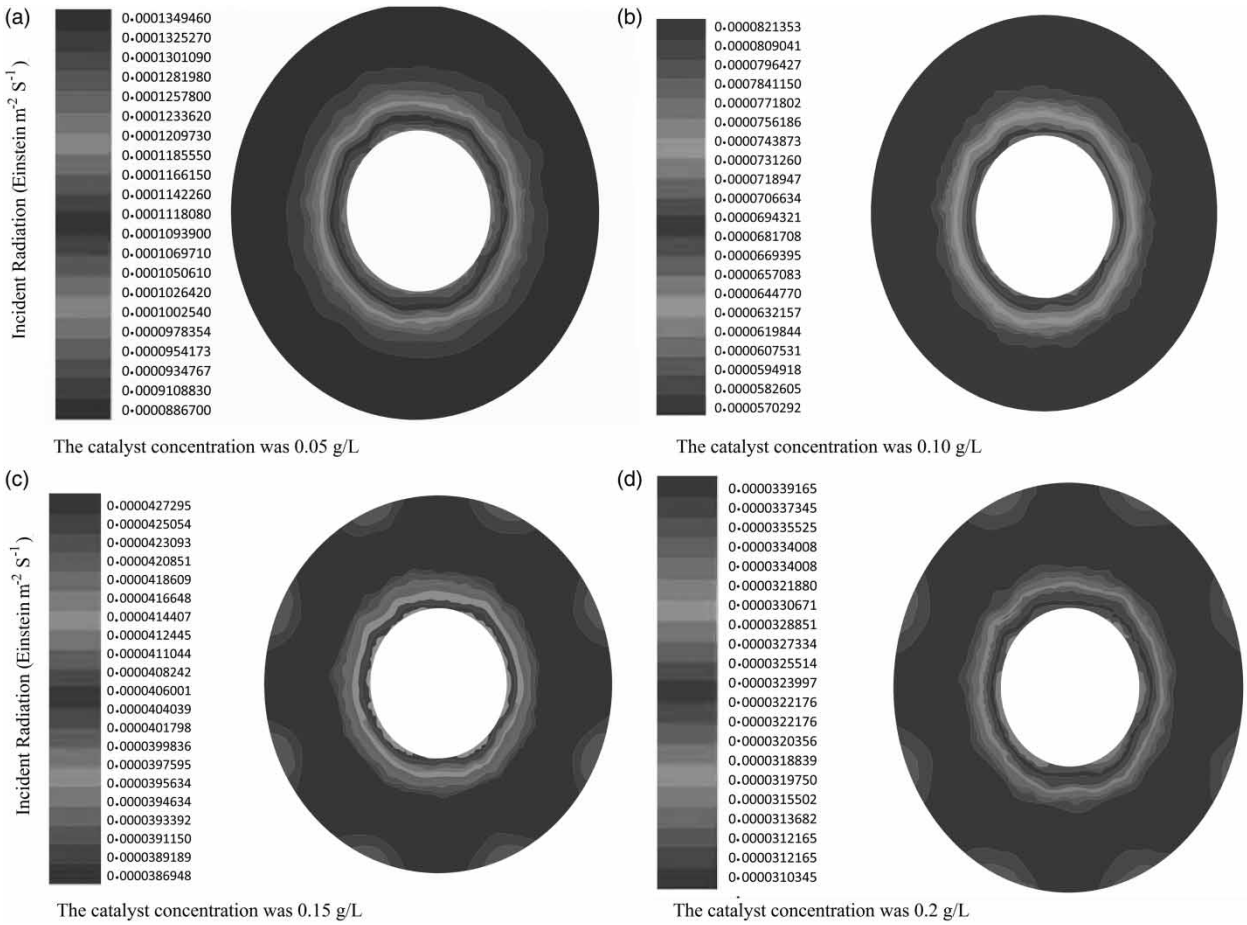

Figure 5 | The incident radiation at various concentrations of the catalyst.

Table 1 | Predicted and observed amounts of LVREA in different concentrations of TiO_2 DP 25

TiO_2 DP 25 (g/l)	$LVREA_{Predicted\ by\ DO}$ (Einstein/m^3s)	$LVREA_{by\ MC}$ (Moreira del Rio 2011) (Einstein/m^3s)	$LVREA_{Observed}$ (Moreira del Rio 2011) (Einstein/m^3s)
0	0	0	0
0.01	0.61×10^{-3}	1.00×10^{-3}	1.50×10^{-3}
0.015	1.43×10^{-3}	1.70×10^{-3}	1.90×10^{-3}
0.03	2.91×10^{-3}	3.20×10^{-3}	3.00×10^{-3}
0.05	2.999×10^{-3}	4.78×10^{-3}	3.50×10^{-3}
0.07	3.32×10^{-3}	5.20×10^{-3}	3.75×10^{-3}
0.10	3.697×10^{-3}	4.83×10^{-3}	3.90×10^{-3}
0.13	3.71×10^{-3}	4.30×10^{-3}	3.85×10^{-3}
0.15	3.998×10^{-3}	3.97×10^{-3}	3.88×10^{-3}
0.20	4.012×10^{-3}	4.00×10^{-3}	3.87×10^{-3}

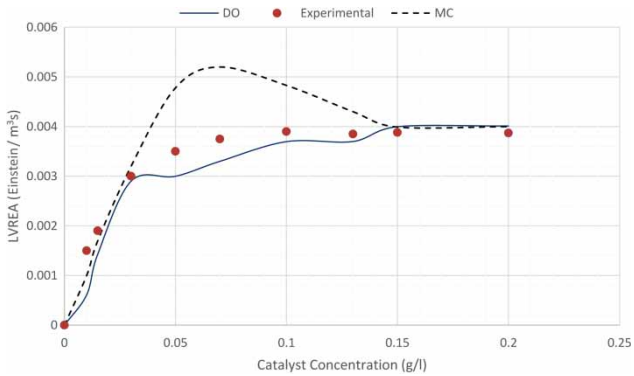

Figure 6 | The LVREA acquired by DO and comparison with MC approaches and experimental data, from Moreira del Rio (2011).

We selected four scenarios with different numbers of tetrahedral cells and nodes to mesh the geometry of the photoreactor and determine the effect of meshing on the

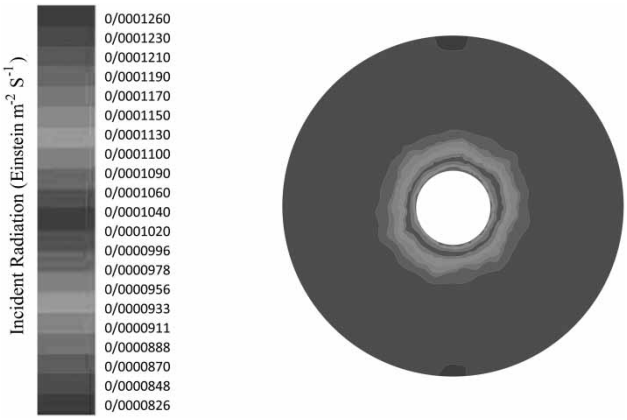

Figure 7 | Effects of geometry of meshing in the photoreactor.

incident radiation by running FLUENT software. For weak meshing, the incident radiation was 0.000126 Einstein/m^2 s (Figure 7) and with strong meshing, the incident radiation was 0.0001349 Einstein/m^2 s (Figure 8). Therefore, meshing the geometry of the photoreactor is important to increase the accuracy of incident radiation predictions.

We compared our work with the study of Elyasi & Taghipour (2010), in which they used the DO method. They did not use the catalyst in their reactor and did not consider the Pyrex sleeve around the lamp for modeling of their radiation. However, we determined the effect of the Pyrex sleeve around the lamp on the amount of LVERA. Asadollahfardi *et al.* (2014) compared the incident radiation of one and two lamps in a photoreactor using the DO method and their results indicated that two lamps instead of one lamp, while the power of two lamps was equal to one, had a better incident radiation than one lamp. Our work was in a heterogeneous photoreactor and their study was in the homogenous photoreactor and ignored the effect of the Pyrex sleeve around the lamps with regard to modeling of radiation.

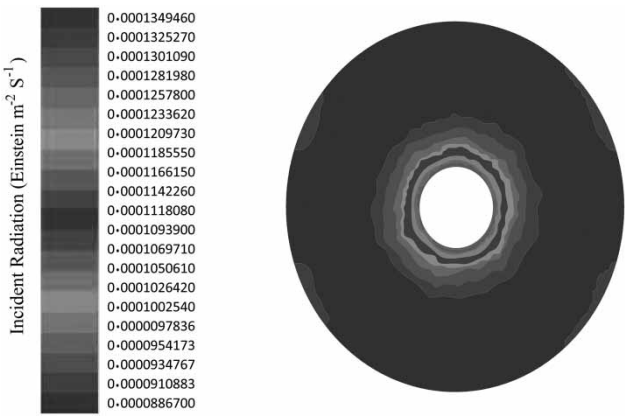

Figure 8 | Effects of geometry of meshing in the photoreactor.

CONCLUSIONS

Considering the solving of the radiation transfer equations in a water treatment reactor, including a UV lamp and DP 25 catalyst, we reached the following conclusions: the LVREA calculations were not sensitive to the Pyrex sleeve; the LVREA values were directly dependent on the catalyst concentrations; the DO method gave satisfactory results in calculation of LVREA. The results were in good agreement with the experimental measurements ($R^2 = 0.95$ and IA = 0.93); the MC method gave satisfactory results in calculation of LVREA. The results were in good agreement with the experimental measurements ($R^2 = 0.91$ and IA = 0.87); up to a concentration of 0.03 g/l as well as concentrations greater than 15 g/l, the MC and DO results had a good convergence with the experimental data; and in spite of the acceptable performance of DO and MC methods in LVREA calculations, the results of DO were more consistent with the observations.

REFERENCES

Asadollahfardi, G., Molaei, M., Taheriyoun, M. & Leversage, I. 2014 Comparison of ultraviolet (UV) radiation intensity between a single lamp and a double lamp in a reactors. *Water Practice and Technology* **9**, 558–565.

Bagheri, M. & Mohseni, M. 2014 Computational fluid dynamics (CFD) modeling of VUV/UV photoreactors for water treatment. *Chemical Engineering Journal* **256**, 51–60.

Bolton, J. R. 2000 Calculation of ultraviolet fluence rate distributions in an annular reactor: significance of refraction and reflection. *Water Research* **34**, 3315–3324.

Brandi, R. J., Citroni, M. A., Alfano, O. M. & Cassano, A. E. 2003 Absolute quantum yields in photocatalytic slurry reactors. *Chemical Engineering Science* **58**, 979–985.

Cassano, A. E., Martin, C. A., Brandi, R. J. & Alfano, O. M. 1995 Photoreactor analysis and design-fundamentals and applications. *Industrial & Engineering Chemistry Research* **34**, 2155–2201.

Crittenden, J. C., Hu, S., Hand, D. W. & Green, S. A. 1999 A kinetic model for H_2O_2/UV process in a completely mixed batch reactor. *Water Research* **33**, 2315–2328.

Elyasi, S. 2009 *Development of UV Photoreactor Models for Water Treatment*. PhD thesis, The University of British Columbia, Vancouver, Canada.

Elyasi, S. & Taghipour, F. 2005 Simulation of a UV photoreactor in the Eulerian framework governing by complex deactivation rate of microorganisms. Third International Congress on Ultraviolet Technologies, Whistler, Canada.

Elyasi, S. & Taghipour, F. 2010 Simulation of UV photoreactor for degradation of chemical contaminants: model development and evaluation. *Environmental Science & Technology* **44**, 2056–2063.

Heckman, J. J. 1979 Sample selection bias as a specification error. *Econometrica: Journal of the Econometric Society* **47**, 153–161.

Ho, C. K. 2009 Evaluation of reflection and refraction in simulations of ultraviolet disinfection using the discrete ordinates radiation model. *Water Science and Technology* **59** (12), 2421–2428.

Imoberdorf, G. & Mohseni, M. 2012 Kinetic study and modeling of the vacuum-UV photoinduced degradation of 2, 4-D. *Chemical Engineering Journal* **187**, 114–122.

Imoberdorf, G. E., Taghipour, F. & Mohseni, M. 2008 Radiation field modeling of multi-lamp, homogeneous photoreactors. *Journal of Photochemistry and Photobiology A: Chemistry* **198**, 169–178.

Jin, S., Linden, K. G., Ducoste, J. & Liu, D. 2005 Impact of lamp shadowing and reflection on the fluence rate distribution in a multiple low-pressure UV lamp array. *Water Research* **39**, 2711–2721.

Kheyrandish, A., Mohseni, M. & Taghipour, F. 2017 Development of a method for the characterization and operation of UV-LED for water treatment. *Water Research* **122**, 570–579.

Krause, P., Boyle, D. P. & Bäse, F. 2005 Comparison of different efficiency criteria for hydrological model assessment. *Advances in Geosciences* **5**, 89–97.

Li, M., Qiang, Z. & Bolton, J. R. 2013 In situ detailed fluence rate distributions in a UV reactor with multiple low-pressure lamps: comparison of experimental and model results. *Chemical Engineering Journal* **214**, 55–62.

Li, W., Li, M., Bolton, J. R., Qu, J. & Qiang, Z. 2017 Impact of inner-wall reflection on UV reactor performance as evaluated by using computational fluid dynamics: the role of diffuse reflection. *Water Research* **109**, 382–388.

Liou, B. T. & Wu, C. Y. 1996 Radiative transfer in a multi-layer medium with Fresnel interfaces. *Heat and Mass Transfer* **32** (1), 103–107.

Liu, D., Ducoste, J. J., Jin, S. & Linden, K. 2004 Evaluation of alternative fluence rate distribution models. *Journal of Water Supply: Research and Technology – AQUA* **53**, 391–408.

Martin, C. A., Baltanas, M. A. & Cassano, A. E. 1996 Photocatalytic reactors II. Quantum efficiencies allowing for scattering effects. An experimental approximation. *Journal of Photochemistry and Photobiology A: Chemistry* **94**, 173–189.

Marugán, J., Van Grieken, R., Alfano, O. M. & Cassano, A. E. 2006 Optical and physicochemical properties of silica-supported TiO_2 photocatalysts. *AIChE Journal* **52**, 2832–2843.

Moreira del Rio, J. 2011 *Photocatalytic Degradation of Phenolic Compounds in Water: Irradiation and Kinetic Modelling*. PhD thesis, The University of Western Ontario, Canada.

Munoz, A., Craik, S. & Kresta, S. 2007 Computational fluid dynamics for predicting performance of ultraviolet disinfection sensitivity to particle tracking inputs. *Journal of Environmental Engineering and Science* **6**, 285–301.

Pareek, V. K., Cox, S. & Adesina, A. A. 2003 Light intensity distribution in photocatalytic reactors using finite volume method. In: *Third International Conference on CFD in the Minerals and Process Industries*, CSIRO, Melbourne, Australia.

Pareek, V., Chong, S., Tadé, M. & Adesina, A. A. 2008 Light intensity distribution in heterogenous photocatalytic reactors. *Asia-Pacific Journal of Chemical Engineering* **3**, 171–201.

Peyton, G. R. & Glaze, W. H. 1988 Destruction of pollutants in water with ozone in combination with ultraviolet radiation. 3. Photolysis of aqueous ozone. *Environment Science and Technology* **22**, 761–767.

Romero, R. L., Alfano, O. M. & Cassano, A. E. 2003 Radiation field in an annular, slurry photocatalytic reactor. 2. Model and Experiments. *Industrial & Engineering Chemistry Research* **42**, 2479–2488.

Salaices, M., Serrano, B. & De Lasa, H. I. 2002 Experimental evaluation of photon absorption in an aqueous TiO_2 slurry reactor. *Chemical Engineering Journal* **90** (3), 219–229.

Sozzi, D. A. & Taghipour, F. 2006 UV reactor performance modeling by Eulerian and Lagrangian methods. *Environmental Science & Technology* **40**, 1609–1615.

Stamnes, K., Tsay, S. C., Wiscombe, W. & Jayaweera, K. 1988 Numerically stable algorithm for discrete-ordinate-method radiative transfer in multiple scattering and emitting layered media. *Applied Optics* **27**, 2502–2509.

Taghipour, F. & Sozzi, A. 2005 Modeling and design of ultraviolet reactors for disinfection by-product precursor removal. *Desalination* **176**, 71–80.

Turolla, A., Santoro, D., de Bruyn, J. R., Crapulli, F. & Antonelli, M. 2016 Nanoparticle scattering characterization and mechanistic modelling of UV–TiO_2 photocatalytic reactors using computational fluid dynamics. *Water Research* **88**, 117–126.

Wols, B. A. & Hofman-Caris, C. H. M. 2012 Review of photochemical reaction constants of organic micropollutants required for UV advanced oxidation processes in water. *Water Research* **46** (9), 2815–2827.

Yokota, T., Cesur, S., Suzuki, H., Baba, H. & Takahata, Y. 1999 Anisotropic scattering model for estimation of light absorption rates in photoreactor with heterogeneous medium. *Journal of Chemical Engineering of Japan* **32**, 314–321.

Zhang, L. & Anderson, W. A. 2013 Kinetic analysis of the photochemical decomposition of gas-phase chlorobenzene in a UV reactor: quantum yield and photonic efficiency. *Chemical Engineering Journal* **218**, 247–252.

First received 10 March 2017; accepted in revised form 16 October 2017. Available online 27 November 2017